Volume 1 | Number 1 | Jan 2013 | Pages 1–100

Dalton Transactions

An international journal of inorganic chemistry
www.rsc.org/dalton

ROYAL SOCIETY OF CHEMISTRY

ROYAL SOCIETY OF CHEMISTRY

www.rsc.org/dalton

Journal Name

Dynamic Article Links ▶

ARTICLE TYPE

New 'Aggregation Induced Emission (AIE)' Active Cyclometalated Iridium(III) Based Phosphorescence Sensors: High Sensitivity for Mercury(II) Ions

Parvej Alam[a], **Gurpreet Kaur**[b], **Clàudia Climent**[c], **Saleem Pasha**[a], **David Casanova**[d], **Pere Alemany**[c]*,
5 **Angshuman Roy Choudhury**[b]*, **Inamur Rahaman Laskar**[a]*

[a]Department of Chemistry, Birla Institute of Technology and Science, Pilani Campus, Pilani, Rajasthan, India, **ir_laskar@bits-pilani.ac.in**; [b]Department of Chemical Sciences, Indian Institute of Science Education and Research (IISER), Mohali, Sector 81, S. A. S. Nagar, Manauli PO, Mohali, Punjab, 140306, India, **angshurc@iisermohali.ac.in**; [c]Departament de Química Física and Institut de Química Teòrica i Computacional (IQTCUB), Universitat
10 de Barcelona. Martí i Franquès 1-11, 08028 Barcelona, Spain, Email: **p.alemany@ub.edu**; [d]Kimika Fakultatea, Euskal Herriko Unibertsitatea (UPV/EHU), Donostia International Physics Center (DIPC), P.K. 1072, 2080 Donostia, Spain; and IKERBASQUE, Basque Foundation for Science, 48011 Bilbao, Spain.

Design and syntheses of 'Aggregation Induced Emission (AIE)' active blue-emitting bis-cyclometalated iridium(III)complexes with appended diphosphine ligands $[Ir(F_2ppy)_2(L_1/L_2)_2(Cl)]$ (F_2ppy=2-(2′,4′-difluoro) phenylpyridine; L_1 = 1,2-bis(diphenylphosphino)ethane; L_2 = bis(diphenylphosphino)propane) have been realized on a suitable route. The free phosphorous donor atom present on the appended
20 diphosphine is shown to provide selective binding to the mercuric ion (Hg^{2+}). The selective binding ability of the probe molecule towards mercuric ions results in a detectable signal due to complete quenching of their AIE property. The quenching effect of the probe molecule has been explored and found to be the resultant of the degradation of the probe iridium(III) complex triggered by the presence of mercuric ion due to an interplay of a soft-soft interaction between the free phosphorous atom of probe
25 molecule with mercuric ions. These complexes were modelled to obtain deeper understanding of excited state properties and the results were tentatively correlated with the experimental data.

30

Dalton Transactions Accepted Manuscript

ARTICLE TYPE

Introduction

Over the past two decades, iridium(III) organometallic phosphors have been found to behave as excellent phosphorescent emitters with a promising potential for applications in flat-panel displays and lighting systems[1]. These iridium(III) compounds have recently attracted also a great interest for the development of new chemosensors[1h] due to their photophysical properties such as long emissive lifetimes, significant Stokes shifts and high quantum yields in the visible region[2].

Mercury is one of the lethal weapons for human health as well as for environment even at very low concentrations[3]. Therefore, the development of different types of sensing systems for monitoring the presence of mercury in environmental samples is drawing a prime attention to the scientific community in recent years[4]. In this context, strong emitting cyclometalated complexes of iridium(III) would be attractive candidates for sensing purposes.

In a recent literature survey, several reports[4, 5] were found where the detection of mercury ions was carried out with taking advantage of the photophysical properties of emissive cyclometalated iridium(III) complexes. In most of the cases, a sulphur atom[5] was strategically incorporated into the complex framework to exploit the preferential binding according to Pearson's soft acid - soft base interactions[6] of sulphur with the soft acid mercuric ion. This phenomenon has been exemplified with systems such as $Ir(btp)_2(acac)$ [5a] (btp = 2-(benzo[b]thiophen-2-yl)pyridine, acacH= acetyl acetone), $Ir(thq)_2(acac)$[4b] (thq=2-(thiophen-2-yl)quinoline). The soft-soft interaction also leads to a protection –de-protection mechanism in $[Ir(pba)_2(bipy)PF_6]$[5c] (Hpba = 4-(Pyridin-2-yl)benzaldehyde; bipy= 2,2′-bipyridine) or to the Hg^{+2}-induced decomposition observed for $Ir(thq)_2(dbm)$[4d] (thq= 2-(thiophen-2-yl)quinoline, dbm= 1,3-diphenylpropane-1,3-dione), $Ir(TBT)_2(acac)$[5d] (TBT=2-thiophen-2-yl-benzothiazole), $[Ir(ppa)(dmppa)\{(Ph_2PS)_2N\}]$[5e] (ppa= 4-phenylphthalazin-1-ol), (dmppa=1-phenoxy-4-phenylphthalazine) $(Ph_2PS)_2N$= bis(diphenylthiophosphoryl)amide), $[Ir(bt)_2(acac)]$[4c] (Hbt = 2-phenylben zothiazole), and $[Ir(ppy)_2(PBT)]$ (PBT= 2-

phenylbenzo[d]thiazole). Hui Zeng *et al.* reported recently the use of $[Ir(pbi)_2(acac)]$[7](pbi= 1,2-diphenyl-1H-benzo[d]imidazole) as a first example of a sulphur free iridium(III) complex used as a highly selective phosphorescent chemosensor for mercuric ions. The detection limit of mercury ions using these types of complexes can be further improved if the system used as probe molecules shows 'aggregation induced emission (AIE)' activity. In the last few years, many organic materials along with several iridium(III) complexes[9] have been identified as AIE active emitters. In most of these cases, the AIE activity has been attributed to restricted intramolecular rotation (RIR) of the rotating units (e.g., phenyl present in triphenylphosphines etc) in the condensed phase.

In this communication, we present the design and synthesis of new cyclometalated iridium(III) complexes where phenyl-substituted diphosphines are used as ancillary ligands with only one phosphorous atom is coordinated to iridium(III) while the other phosphorous unit remains non-coordinated to the chromophoric iridium(III) unit and can, thus, be potentially utilized for selective sensing of metal ions. The synthesized complexes show AIE activity and have been shown to act as a promising Hg^{2+} sensors. In addition, the excited state properties of these complexes were studied using DFT-based quantum chemical calculations.

Experimental Section

Materials

Iridium(III) chloride hydrate, 1,2-Bis(diphenylphosphino)ethane (L_1), Bis(diphenylphosphino)propane (L_2) and 2-ethoxyethanol were purchased from Sigma Aldrich Chemical Company Ltd. 2-(2,4-Difluorophenyl) pyridine (F_2ppy) and $[Ir(F_2ppy)_2Cl]_2$ bridge complex were prepared according to a reported procedure[11]. The UV-VIS grade solvents (DCM, hexane, ethyl acetate) and metal nitrate salts were procured from Merck Company.

General Synthesis of 1 and 2

In a two-necked round bottom flask (50 ml), diphosphine ligands

[L$_1$/L$_2$] (0.087 mmol) and ([dfppy)$_2$Ir(μ-Cl)]$_2$ (0.087 mmol) were dissolved in 20 mL DCM. The mixture was stirred at room temperature for 2 minutes under an atmosphere of N$_2$ gas. The solution mixture was evaporated to dryness and the residue purified by column chromatography using DCM-Hexane (30:70) as the eluent, getting a green solid product (**Scheme 1**). ^{1}H NMR (400 MHz, CDCl$_3$) δ 9.43 (d, J = 5.9 Hz, 1H), 8.83 (d, J = 4.8 Hz, 1H), 8.35 (dd, J = 8.2, 2.4 Hz, 1H), 7.90 (t, J = 8.2 Hz, 1H), 7.79 (t, J = 8.0 Hz, 1H), 7.73 – 7.58 (m, 2H), 7.60 – 7.45 (m, 3H), 7.45 – 7.13 (m, 13H), 7.06 (td, J = 7.9, 2.1 Hz, 2H), 6.98 – 6.82 (m, 3H), 6.80 – 6.71 (m, 1H), 6.38 (ddd, J = 12.7, 9.0, 2.3 Hz, 1H), 6.25 – 6.13 (m, 1H), 5.59 (dd, J = 9.0, 2.0 Hz, 1H), 5.30 (ddd, J = 8.2, 5.6, 2.4 Hz, 1H), 2.78 – 1.91 (m, 2H), 1.89 – 1.66 (m, 2H). ^{19}F NMR (376 MHz, CDCl$_3$) δ -107.36, -107.38, -107.39, -107.41, -107.51, -107.53, -107.54, -107.56, -108.13, -108.14, -108.15, -108.16, -109.78, -109.81, -109.83, -109.87, -109.89, -109.92, -110.01, -110.04, -110.13, -110.16. ^{31}P NMR (162 MHz, CDCl$_3$) δ -8.90, -8.95, -9.00, -9.10, -9.15, -9.20, -12.07, -12.27, -12.67. Anal. calcd for C$_{48}$H$_{36}$ClF$_4$IrN$_2$P$_2$: C, 57.28; H, 3.61; N, 2.78; Found: C, 57.10; H, 3.57; N, 2.75; HRMS calculated: ([M-Cl]$^+$): m/z 971.1919 found: ([M-Cl]$^+$), m/z 971.1892; Green solid; Yield 68.49% for **1**. ^{1}H NMR (400 MHz, CDCl$_3$) δ 9.45 (d, J = 5.5 Hz, 1H), 8.74 (d, J = 5.6 Hz, 1H), 8.33 (dd, J = 7.7, 3.2 Hz, 1H), 7.96 (dd, J = 32.1, 8.5 Hz, 1H), 7.82 – 7.57 (m, 3H), 7.57 – 7.39 (m, 4H), 7.39 – 7.19 (m, 10H), 7.05 (m, 7H), 6.66 (dt, J = 12.1, 6.4 Hz, 1H), 6.38 (ddd, J = 12.7, 9.1, 2.2 Hz, 1H), 6.31 – 6.10 (m, 1H), 5.61 (ddd, J = 14.8, 8.9, 1.9 Hz, 1H), 5.40 – 5.23 (m, 1H), 2.68 (m, 2H), 2.31 – 2.05 (m, 2H), 2.03 – 1.77 (m, 2H) . ^{19}F NMR (376 MHz, CDCl$_3$) δ -107.46, -107.48, -107.48, -107.50, -107.53, -107.54, -107.55, -107.57, -107.59, -108.22, -108.25, -108.35, -108.38, -109.83, -109.85, -109.88, -109.91, -109.93, -109.97, -110.00, -110.13, -110.15. ^{31}P NMR (162 MHz, CDCl$_3$) δ -12.43, -12.94, -12.99, -13.04, -17.56, -18.27. Anal. calcd for C$_{49}$H$_{38}$ClF$_4$IrN$_2$P$_2$: C, 57.67; H, 3.75; N, 2.75; Found: C, 57.50; H, 3.70; N, 2.68, HRMS calculated: ([M-Cl]$^+$): m/z 985.2076 found: ([M-Cl]$^+$), m/z 985.2066; Green solid; Yield 54.79% for **2**.

Synthesis of 3

Complex **2** (equimolar) and [dfppy$_2$Ir(μ-Cl)]$_2$ were added in stirred solution of DCM at room temperature for 5 minutes. The product was purified using 60-120 mesh silica gel, DCM as eluent, getting a green product (**Scheme 1**).

^{1}H NMR (400 MHz, CDCl$_3$) δ 9.43 (d, J = 6.0 Hz, 1H), 9.30 (d, J = 5.8 Hz, 1H), 8.56 (d, J = 5.8 Hz, 2H), 8.31 (dd, J = 7.9, 4.2 Hz, 2H), 7.96 (d, J = 8.6 Hz, 1H), 7.88 (d, J = 8.6 Hz, 1H), 7.76 – 7.60 (m, 5H), 7.31 (d, J = 8.3 Hz, 6H), 7.19 (ddd, J = 18.4, 15.3, 8.1 Hz, 5H), 7.10 – 6.99 (m, 3H), 6.99 – 6.84 (m, 1H), 6.80 (t, J = 8.3 Hz, 3H), 6.49 (t, J = 6.1 Hz, 1H), 6.37 (ddd, J = 13.6, 5.5, 2.2 Hz, 3H), 6.28 – 6.14 (m, 1H), 5.59 (dd, J = 8.9, 2.0 Hz, 1H), 5.52 (dd, J = 8.8, 1.9 Hz, 1H), 5.27 (tdd, J = 8.2, 5.7, 2.3 Hz, 2H), 2.61 – 2.28 (m, 4H), 1.78 (d, J = 6.0 Hz, 2H), ^{31}P NMR (162 MHz, CDCl$_3$) δ - 11.96, -12.46. HRMS calculated: ([M-C$_{22}$F$_4$N$_2$ClIr]$^+$): m/z 1021.1842 found: ([M-C$_{22}$F$_4$N$_2$ClIr]$^+$ m/z 1021.1831 .

Synthesis of 4

Hg(NO$_3$)$_2$ (4 moles) was added to a stirred solution of **2** (1 mole) dissolved in a mixture of water and DMF (7 : 3). The reaction was completed i n very short period of time (~1 minute). The reaction mixture was washed by cold water and extracted by DCM. The organic layer was dried over Na$_2$SO$_4$ and evaporated under reduced pressure resulting in a light yellow product (Scheme 2). ^{1}H NMR (400 MHz, CDCl$_3$) δ 8.76 (d, J = 5.6 Hz, 2H), 8.33 (d, J = 8.4 Hz, 2H), 7.97 (t, J = 7.7 Hz, 2H), 7.41 – 7.37 (m, 2H), 6.44 (ddd, J = 11.8, 9.2, 2.3 Hz, 2H), 5.51 (dd, J = 8.7, 2.2 Hz, 2H), 1.67 (s, 6H). ^{19}F NMR (376 MHz, CDCl$_3$) δ -107.07, -109.72. Anal. calcd for C$_{22}$H$_{16}$ClF$_4$IrN$_2$O$_2$: C, 41.03; H, 2.50; N, 4.35; Found: C, 40.51; H, 2.79; N, 4.32, HRMS calculated: ([M-2H$_2$O]$^+$), m/z 573.0566 and ([M-2H$_2$O+ACN]$^+$): m/z 614.0831 found: ([M-2H$_2$O]$^+$), ([M-2H$_2$O+ACN]$^+$) : m/z 614.0826, Light yellow solid; Yield 16.00% for **4**.

Characterization

^{1}H NMR, ^{13}C NMR, ^{19}F and ^{31}P NMR spectra were recorded in a 400 MHz Brucker spectrometer using CDCl$_3$ as solvent and tetramethylsilane (TMS, δ = 0 ppm for ^{1}H and ^{13}C NMR), Trifluoro acetic acid (CF$_3$COOH, δ = 0 ppm for ^{19}F NMR) and phosphoric acid (H$_3$PO$_4$, δ = 0 ppm for ^{31}P NMR) as internal standard. Infra-red spectra were recorded in a FTIR Simadzu (IR prestige-21) and a Perkin Elmer Spectrum 100 FTIR spectrometer. UV-VIS absorbance spectra were recorded using a Simadzu Spectrophotometer (model UV-1800 and 2550). The steady state photoluminescence spectra were recorded on

Spectrofluorometer FLS920-s Edinburgh. The solid state quantum yield of the thin film sample was measured using a calibrated integrating sphere in a Gemini spectrophotometer (Gemini 180). Elemental analyses were furnished on Elementar, 5 VARIO III. Particle sizes of the nano-aggregates were determined using a Malvern Zetasizer (MAL1040152). Microwave reactions were carried out in a CEM Discover (mode l908010). All the reactions were performed under nitrogen atmosphere and the progress of the reaction was monitored using 10 thin-layer chromatography (TLC) plates (pre-coated with 0.20 mm silica gel).

Fabrication of thin-film substrate for PL measurements

10^{-3}M solutions of **1** and **2** in DCM were prepared. 2-3 drops of 15 these solutions were placed on a thin glass substrate ($2 \times 2 \text{cm}^2$) and the solvent was allowed to evaporate slowly.

Computational Details

20 Ground state geometry optimizations were performed within density functional theory (DFT) using the B3LYP hybrid functional[12]. A basis set of double-ζ quality (LANL2DZ) and the effective core potential of Hay and Wadt were used for Iridium, whereas a 6-31G(d) basis set was used for the rest of the atoms[13]. 25 In order to describe the electronic transitions to the low lying singlet and triplet states, time-dependent density functional theory (TD-DFT) calculations were carried out with the same functional and basis sets. All calculations were performed in dichloromethane ($\varepsilon=8.93$) using the Integral Equation Formalism 30 - Polarizable Continuum Model (IEF-PCM) for the solvent and the Gaussian 09 package.

Scheme 1 Schematic presentation of synthetic protocol for the complexes of **1, 2** and **3**

A

n=2 ⟶ Complex 1
n=3 ⟶ Complex 2

n=3 ⟶ Complex 3

A

DCM,RT / 5 min
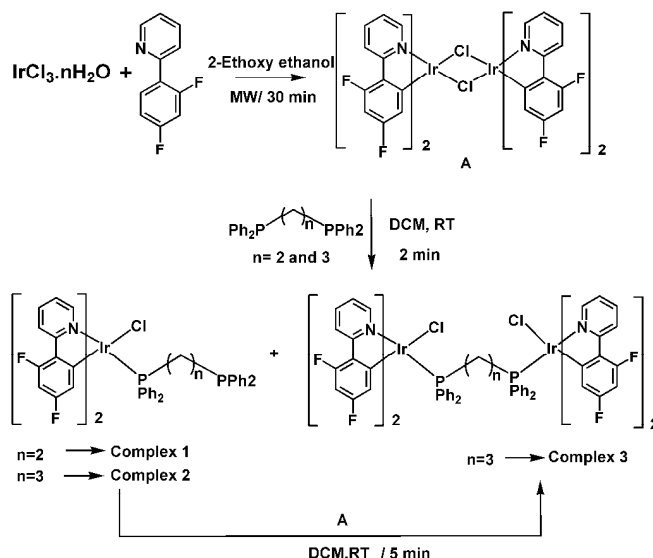
Results and Discussion

Syntheses

Blue emitting phosphorescent transition metal complexes are 40 usually being synthesized employing a wide-energy-gap cyclometalated ligand, such as 4,6-difluorophenyl pyridine (dfppyH), 3-trifluoromethyl-5-(2-pyridyl) pyrazole and many other functionalized cyclometalates[10a,b]. The electron with-drawing fluoro substituents which are located at the meta-45 positions with respect to the central metal atom, stabilize the metal d_{π} orbitals[10c], while strong-field ligands such as cyanide or phosphines directly bonded to metal are found to be capable of increasing the band gap.

Several new blue-emitting complexes were synthesized (Scheme 50 1) using a strong-field ligand with phosphorous-donating diphosphine ligands. In these cases, diphosphines are coordinated to bis-cyclometalated iridium(III) complex in a monodentated mode while the other donating phosphines remain as appended with the possibility of coordinating to another metal. This idea 55 was originated from our previous report[14] where [(ppy)$_2$Ir(μ-Cl)$_2$Ir(ppy)$_2$] (ppy = 2-phenyl pyridine) was reacted with diphosphine ligands (L$_1$/L$_2$), resulting a chelate complex of diphosphine [Ir(ppy)$_2$(PPh$_2$CH$_2$CH$_2$PPh$_2$)]PF$_6$. This was obtained as the absolute product even lowering the temperature to room 60 temperature. For the syntheses of the compounds described in this report, the chloro-bridged dinuclear iridium(III) complex, [(F$_2$ppy)$_2$Ir(μ-Cl)$_2$Ir(F$_2$ppy)$_2$] (F$_2$ppy=2-(2′,4′-difluoro)phenylpyridine) and diphosphine ligands (L$_1$/L$_2$) were

reacted in dichloromethane at room temperature for very short periods (2 minutes). The synthesized complexes exhibit an intense blue emission under excitation by UV ray with a fascinating structure where the diphosphine coordinate as monodentate to the central metal atom. Probably, the presence of strong electronegative fluorine atoms in phenyl of 2-phenylpyridine restricts the formation of chelating complex of diphosphine to iridium(III) in these cases. With using bis(diphenylphosphino)propane (L_2) as diphosphine, the crude reaction mass contains two products that were isolated by column chromatography (**2** and **3**).   The complex **2** corresponds to the appended diphosphine in bis-2-(2′,4′-difluoro)phenylpyridine iridium(III) complex (**Scheme 1**). The complex **3** was characterized which corresponds to $[(F_2ppy)_2Ir(\mu-L_2)Ir(F_2ppy)_2]$. On the other hand, for the case of 2-bis(diphenylphosphino)ethane (L_1), the exclusive formation of the complex which corresponds to bis-2-(2′,4′-difluoro)phenylpyridineiridium(III) where diphosphine ligand remains as appended (mono coordinated) (**1**) at   room temperature (**Scheme 1**). It is to be noted that there has no formation of chelating diphosphine iridium(III) complex in this case, even upon allowing the reaction to continue for 72h. The chelating diphosphine mixture was isolated when the reaction mixture was refluxed in methanol for 15 min. This observation depicts the occurrence of chelating / or non-chelating which is absolutely depending upon temperature variation. We have isolated and characterized the chelating complex by ^1H NMR and HRMS and results are given in supporting document (Fig. S1).

The ^1H, ^{31}P and ^{19}F NMR spectra of these complexes support that the structure of complexes **1** and **2** contains a free terminal phosphine group (**Fig. S2** and **S3**) whereas **3** (**Fig S4**) is a bimetallic iridium complex with the diphosphine ligand acting as a bridge between the two iridium(III) centers. The isolation of **3** from the reaction mixture indirectly supports the monodentate rather than chelating coordination mode of diphosphines to iridium in **1** and **2** (Scheme 1). The synthesized complexes have C1 symmetry, and as a consequence, the results show a ^1H NMR spectrum where the total number of proton resonances equals the total number of aromatic protons present in the complex. The ^1H NMR data of **1** and **2** show **12** distinct sets of aromatic protons which correspond to the total number of protons present in the complexes (**Fig. S2** and **S3**).

In the ^{31}P-$\{^1H\}$-NMR spectrum of **1** and **2**, the presence of two clearly non-equivalent P atom peaks supports the fact that one of the phosphorous atoms remains without coordination in the complex. The ^{31}P signal of the coordinated phosphorous atom appears as a double triplet (dt) at δ -9.2 ppm with J_{P-F} = 8.1 Hz, whereas the non-coordinated phosphorous atom shows a peak corresponding to a double singlet signal at δ -12.2 ppm with J_{P-P}= 31.5 Hz which matches well with previous reports[15](**Fig 1**) for free PPh_2. Each phosphorous signal will split into a doublet[16] and signal "a" (db signal) will split further into a triplet by P-F coupling while signal "b" will not split further because of weak long range coupling. Similarly, for the case of **2**, the ^{31}P-$\{^1H\}$-NMR spectrum shows two different signals: the one labelled as "a", a triplet at δ -12.9 ppm with J_{P-F} =7.7 Hz and a signal "b" appearing as a singlet. In this case, since there should be no splitting between two P atoms (because of the long range coupling), they should appear both as singlets, but signal "a" will be further split by interaction with the F atom into a triplet with $J_{P-F} \sim$ 8 Hz. The ^{31}P-$\{^1H\}$-NMR of complex **3** is showing again two different signals "a" and "b", as a double triplet at δ -11.96 ppm and δ -12.46 ppm with J_{P-F} = 8 Hz.
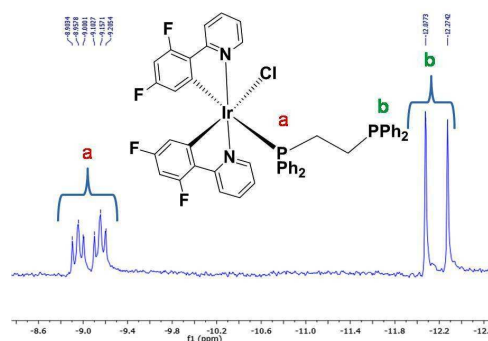
Aggregation-Induced Enhanced Emission.

The 'aggregation induced emission (AIE)' property of the blue phosphorescence at λ_{max} 461 and 488 nm for both (**Table S1**) complexes, respectively, is investigated. Both compounds are highly soluble in common organic solvents such as dichloromethane (DCM), chloroform ($CHCl_3$), tetrahydrofuran (THF), dimethyl sulfoxide (DMSO) or dimethyl formamide (DMF) but they are not soluble in water. These complexes show a very weak emission only in DMF, but they are both strongly

emissive in the solid state (under illumination with a 365 nm UV lamp). A different amount of water (f_w in the range 0-99%) is gradually added to a set of solutions of complexes **1** and **2,** keeping the overall concentration of the solution to 10^{-5} M. The measured photoluminescence (PL) intensity of complex **1** diminishes up to a water concentration about $f_w \leq 50\%$ [$\leq 60\%$ for **2**], then starting to increase for water fractions up to $f_w = 70\%$ (**Fig. 2a**). At this condition, the PL intensity is about 4 times (3.5 times for **2**) higher than the PL intensity measured in pure DMF solution (**Fig. 2** and **Fig S5**). After reaching a maximum intensity at $f_w = 70\%$, the PL intensity decreases along with increasing water content. The solid state emission intensity of **1** becomes six fold higher than that in pure DMF solution (**Fig. S6**). Similarly, the emission intensity of **2** is about twenty times higher than that in pure DMF solution (**Fig. S6**). We have performed another experiment: with an increasing fraction of polyethylenene glycol (f_{PEG}) in dimethylformamide solutions of definite concentration of **1**, the emission intensity gradually increases (**Fig.S7**). In the viscous PEG medium, the rotation of diphenyl rotors of diphosphine ligand is highly restricted resulting in an emission enhancement. These experiments primarily support the AIE activity of these complexes. At lower percentages of water (f_w, 0-40% for **1** and f_w, 0-50% for 2), the lowering of the PL intensity seems to be due to the formation of amorphous aggregates or to interactions with solvent molecules[17]. In the case of **1**, the PL intensity again decreases after reaching a maximum at 70%. This abnormal variation of the AIE property for both complexes may be due to two reasons. Only those molecules which are present on the surface of nano particles, emit light and contribute to the fluorescent intensity upon excitation, leading to a decrease in the fluorescence intensity after aggregation. On the other hand, the RIR (restricted intermolecular rotations) of substituted phenyl rings at phosphorous around the single bonds in the aggregated state will enhance light emission. The emission intensity of aggregated species will depend on which of both phenomena is going to dominate and affect the fluorescent behaviour of the aggregated molecules after addition of water; the other reason, the solute molecules can aggregate into two kinds of nanoparticle suspensions: crystalline and amorphous particles. Crystalline particles would enhance the PL intensity, while amorphous ones lead to a reduction in the intensity[18,19]. The aqueous mixtures with higher f_w for which the formation of precipitate is not observed, suggests that the size of the aggregates are in the nano-

scale dimension. This is proved by UV-VIS spectra of the complexes having the level-off tail in the longer wavelength region (400-650 nm) (**Fig S8**). The PXRD data of **1** and **2** showed semi-crystalline and amorphous nature, respectively (**Fig. S10**). This observation is in accordance with the observation of maximum PL intensity which was obtained for **1** with water fraction (f_w) 70%.

The solution quantum efficiencies of the complexes **1** and **2** have been measured to 0.067 % and 0.020 %, respectively [reference is used quinine sulphate in 0.1M sulphuric acid, quantum yield (QE) = 0.55]. The absolute solid state QE for the complexes **1** and **2** has been measured using integrating sphere and the values obtained 7.252% and 6.165 %, respectively. So, these QEs are 107 and 295 times higher as compared to their solution quantum efficiencies, respectively in agreement with the strong emission observed in the solid state with respect to their respective solutions showing the remarkable AIE property of the complexes. Life time data for complexes in solution and solid state were found to be 19.30 ns and 2 µs for **1,** and 55.19 ns and 3.382 µs for **2** (**Fig. S10**, **Table S1**), respectively.

Studies using a particle size analyzer also reveal the formation of nanoaggregates (in 90% water fraction) with diameters in the range of 170–200 nm (**Fig. S11**). Clearly, aggregate formation has enhanced the PL of both complexes, in other words, both complexes are AIE-active. The photo physical properties of complex **3** have been studied and found similar emission and absorption bands as those observed for complexes **1** and **2** (**Fig S12**, **Table S1**).
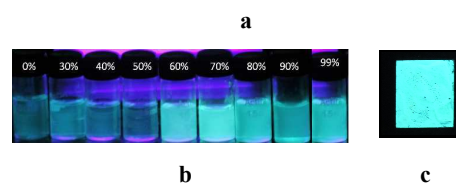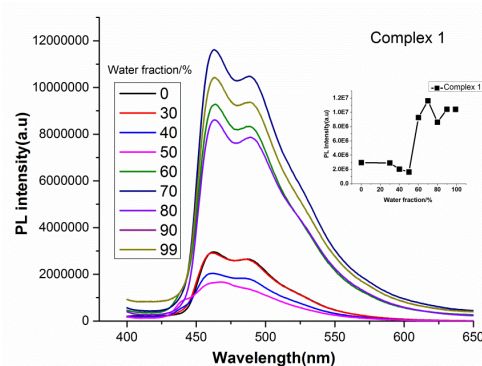

a

b   c

Fig. 2 (**a**) PL spectra of complex **1** with [M] =10^{-5} mol L^{-1} in DMF–water mixtures water fractions (f_w). (**b**) Fluorescent photos of the aqueous mixtures radiated with an ultraviolet light at 365 nm. (**c**) Solid thin film emission of complex **2**

Table 1. Vertical excitation energies, oscillator strengths, and orbital contributions (≥5 %) to the electronic transitions calculated for the transition to lowest excited states of the studied complexes.

	States	ΔE, eV (nm)	f	Assignments
Complex 1	T_1	2.87 (432)		HOMO-4→LUMO (10%)
				HOMO-3→LUMO+1 (8%)
				HOMO-→LUMO+1(14%)
				HOMO → LUMO (48%)
	T_2	2.89 (430)		HOMO-4→LUMO+1 (8%)
				HOMO-3 → LUMO (8%)
				HOMO-2→ LUMO (21%)
				HOMO-2→LUMO+1 (5%)
				HOMO→LUMO+1 (39%)
	S_1	3.26 (380)	0.037	HOMO → LUMO (95%)
	S_2	3.32 (373)	0.004	HOMO→LUMO+1 (95%)
	S_4	3.72 (333)	0.049	HOMO-2→ LUMO (26%)
				HOMO-2→LUMO+1 (47%)
				HOMO-1 → LUMO (5%)
				HOMO-1→LUMO+1 (9%)
Complex 2	T_1	2.84 (436)		HOMO-4→ LUMO (15%)
				HOMO → LUMO (60%)
	T_2	2.89 (428)		HOMO-3 → LUMO (6%)
				HOMO-3→LUMO+1 (13%)
				HOMO-2 → LUMO (7%)
				HOMO-2→LUMO+1 (18%)
				HOMO→LUMO+1 (38%)
	S1	3.19 (389)	0.032	HOMO → LUMO (97%)
	S2	3.33 (373)	0.004	HOMO→LUMO+1 (96%)
	S4	3.75 (331)	0.043	HOMO-2→LUMO+1 (85%)
				HOMO-3→LUMO+1 (5%)

Ground State Geometries

The optimization of the molecular structure for the ground state suggests slightly distorted octahedral coordination geometries for the two Iridium(III) complexes **1** and **2** (**Fig 3**). As shown in **Table S2**, there has no major difference neither in the Ir-X distances nor in the X-Ir-X angles between **1** and **2** except for the Ir-P distance and the Cl-Ir-P angle, whose values increase slightly as the bridge between the two diphenylphoshines becomes larger. In the two structures shown (**Fig. 3),** It is evident that only one of the two phosphorus atoms of the diphosphine belongs to the coordination environment of the iridium atom, while the other one remains free to coordinate with other metal atoms present in the solution.
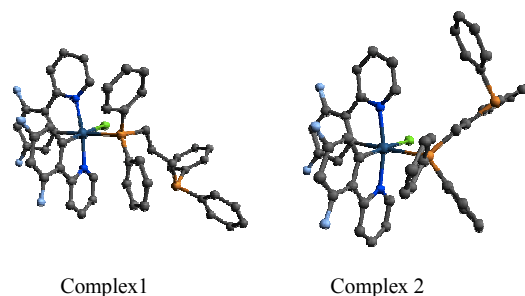

Complex1   Complex 2

Fig. 3 Ground state molecular structures calculated in dichloromethane solution. Hydrogen atoms are not displayed for the sake of clarity.

Frontier Molecular Orbitals

The frontier molecular orbitals of complex **1** are shown (**Fig. 3**). While the HOMO-3, HOMO-2 and HOMO have a remarkable d contribution from the Iridium(III) center, along with a p orbital from the Cl atom and π character from the two 2-phenylpyridine ligands, the HOMO-1 consists on a π type orbital located on one of the diphenylphoshines. The latter one is the only frontier molecular orbital which has participation from the ancillary ligand. The LUMO and LUMO+1 are quasi-degenerate orbitals composed of π* type orbitals located on the 2-phenylpyridine ligands, with no significant metal participation.

Except for the HOMO-1 and HOMO-3, all the other mentioned orbitals have a notable participation in the low-lying electronic states. The relevant molecular orbitals related to the electronic transitions and the HOMO-LUMO gap of approximately 4.0 eV are quite similar for the two studied complexes (see **Table S3**).
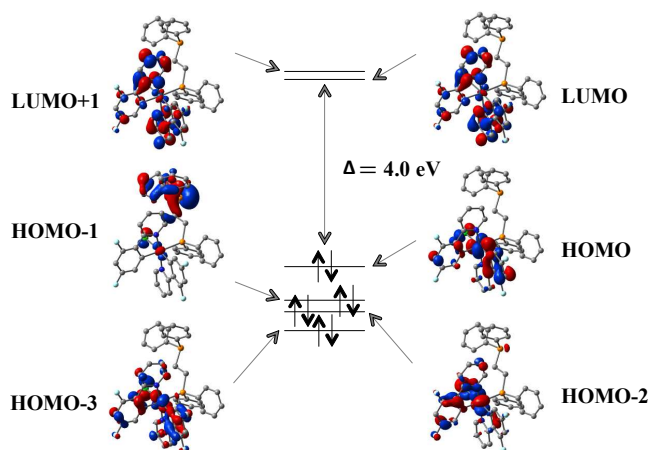
Fig 4. Highest and lowest occupied molecular orbitals for complex **1**.

Excited States

The calculated excitation energies (**Table 1**) corresponding to the electronic transition from the ground state to the first excited singlet state S_1 are 3.26 and 3.19 eV, respectively. This electronic transition can be seen as a promotion of an electron from the HOMO to the LUMO, with an important MLCT character from the d orbitals of the Iridium atom to the π system of the two 2-phenylpyridine ligands, together with some charge transfer from the p orbital of the Cl atom to the two 2-phenylpiridines and a significant π to π^* transition within these ligands. The slightly smaller HOMO-LUMO gap obtained for complex 2 (3.95 vs. 4.04 eV) is responsible for the lower excitation energy calculated for this complex. This information correlates satisfactorily with the experimental absorption spectra. The associated computed oscillator strengths predict similar absorption intensities for the two complexes, in good agreement with the experimental observations.
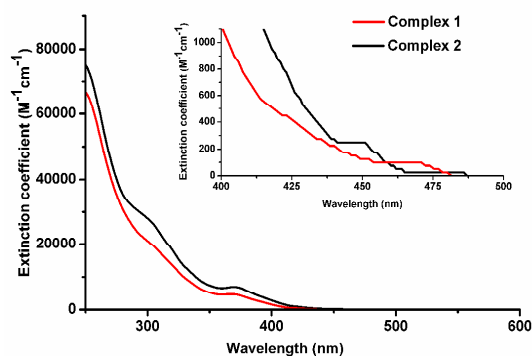

Fig 5. Solution absorption spectra for 1 and 2 at a concentration of 10^{-5}M in DCM (Inset: enlarged absorption spectra in the region 400-500 nm).

In order to gain more insight into the nature of the electronic transitions observed in the experimental absorption spectra, excitations to other low-lying singlet and triplet states were calculated. This information is summarized in **Table 1**. The excitation from the ground state to the second excited singlet state, S_2, is mainly an HOMO to LUMO+1 transition. The nature of this second excited singlet state is quite similar to that of the first excited singlet state because of the resemblance between the LUMO and LUMO+1, although the corresponding oscillator strength for this transition is almost negligible for the two complexes. The intense absorption band observed in the experimental spectra at 300-330 nm (**Fig. 5**) corresponds mainly to the electronic transition to the fourth excited singlet state (with contributions from other high-lying singlet states). The major contribution to this fourth singlet state is an excitation from the HOMO-2 to the LUMO or LUMO+1, with an important MLCT character as it is found for the first singlet state. In the low energy region of the absorption spectra (400-450nm) (**Fig.5**), a band of low intensity is observed which can be attributed to the partially allowed transitions to low-lying triplet states due to the spin-orbit coupling induced by the presence of the metal centre. The calculated excitation energies to the first and second triplet states are in excellent agreement with those found for the experimental absorption bands (**Table S1**). The character of the transitions from the ground state (S_0) to the first and fourth excited singlet (S_1, S_4) and the first triplet states (T_1) has been analyzed comparing the atomic Mulliken populations for each fragment in the molecule. The results shown in **Table S5** indicate very similar MLCT character for the two complexes for the excitations to S_1 and S_4, while the MLCT character play a minor role in the transition to the first excited triplet state T_1.

The nature of the MLCT character of these transitions can be further visualized by plotting the difference between the charge densities of the two states involved in the transition. **Fig. 6** shows these difference plots for complex **1**. From this representation it can be easily seen that the most important charge transfer in the $S_0{\rightarrow}S_1$ and $S_0{\rightarrow}S_4$ transitions, responsible for the absorption process, is between the Iridium atom and one of the two 2-phenylpyridine rings. Very similar plots can be obtained for complex **2**.

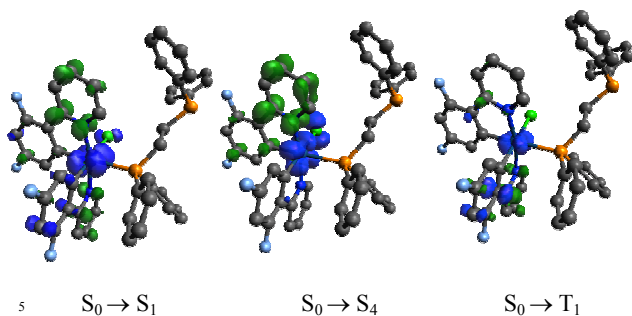$$S_0 \rightarrow S_1 \qquad S_0 \rightarrow S_4 \qquad S_0 \rightarrow T_1$$

Fig 6. Electron density differences between the S_1 and the S_0 states (left), S_4 and S_0 states (middle), and T_1 and S_0 states (right) for complex **1**. Blue corresponds to negative values (higher electron density in the ground state) while green corresponds to positive ones (higher electron density in the corresponding excited state).

**Selective optical response to various metal ions along with Hg^{+2}**

AIE active complexes with appended phosphorous donating atoms such as **1** and **2** have a great potentiality in sensing applications. The emission spectra of **1** in presence of individually different metal ions such as Mg^{2+}, K^+, Ni^{2+}, Al^{3+}, Cd^{2+}, Co^{2+}, Pb^{2+}, Bi^{2+}, Fe^{2+}, Ag^{+1}, Cu^{2+}, Au^{+3}, Zn^{+2} with Hg^{+2} were recorded (the solution giving AIE property is prepared **1** in $DMF/H_2O = 3/7$) (**Fig. 7a**). As it can be seen in (**Fig. 7a-7c**), the emission intensity was ~80 % quenched in the presence of Hg^{+2} ions. The specificity of the probe molecules towards Hg^{+2} ions has been studied in competitive experiments in the presence of other metal ions (**Fig. 7b**). The grey bars represent the intensity of the emitted radiation in presence of Hg^{+2} ions in solution together with individual metal ions such as Mg^{2+}, K^+, Ni^{2+}, Al^{3+}, Cd^{2+}, Co^{2+}, Pb^{2+}, Bi^{2+}, Hg^{+2}, Fe^{2+}, Ag^+, Cu^{2+}, Au^{+3}, and Zn^{+2} showing the high impact on the emission intensity when compared to the black bars which correspond to the emission intensity of a solution of the same metal ion in absence of Hg^{+2}. The quenching effect on the emission intensity of **1** in presence of Hg^{+2} shows that it is a highly selective ratiometric luminescent molecular probe for the detection of Hg^{+2} ions in solution. The experiment performed with **2**, showed similar results (**Fig. S13**). The absorption spectra of **1** were also recorded in presence of different cations, showing a gradual variation of the absorption spectra (**Fig. S14**)].
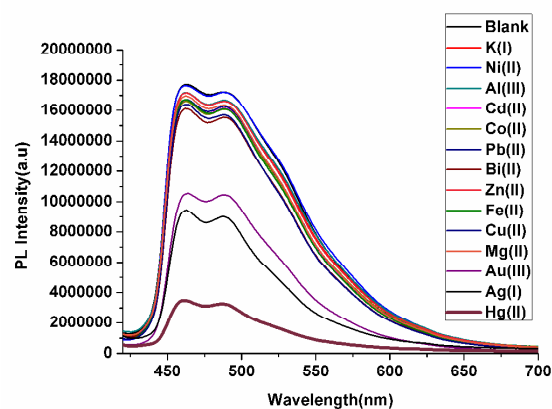

a
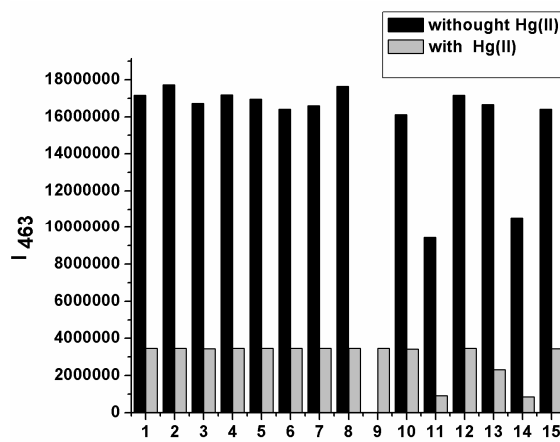
b
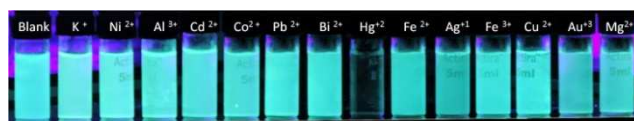
c

Fig. 7(a) Fluorescence spectra of complex 1 with [M] =10^{-5} mol L^{-1} at f_w = 70 % upon the addition of 4 equivalent of metal ions. (**b**) Column diagrams of the fluorescence intensity of complex 1 + M^{n+} at 463 nm. Black bars represent the addition of various metal ion to the blank solution and gray bars represents the subsequently addition of Hg^{+2}(4 equivalent) to the above solutions (complex 1+ M^{n+}+ Hg^{+2}) (**c**) photo of complex 1 when dispersed at f_w = 70 % with [M] =10^{-5} mol L^{-1}, by adding 4 equivalent of metal ions. From left to right: 1,blank ; 2, K^+; 3, Ni^{+2}; 4,Al^{+3}; 5,Cd^{+2} ; 6, Co^{+2}; 7, Pb^{+2}; 8,Bi^{+2}; 9, Hg^{+2};10, Fe^{+2}; 11,Ag^+; 12, Cu^{2+}; 13, Fe^{+3}; 14, Au; and 15, Mg^+ radiated with an ultraviolet light at 365 nm.

The effect of Hg^{+2} on solutions containing complex **1** was also studied very carefully by UV-VIS absorption and PL spectroscopy. Some changes in the UV-VIS absorption spectrum have been observed after titrating **1** with Hg^{+2}: the band at 372 nm which is assigned to the spin-allowed metal-to-ligand charge-transfer (^{1}MLCT) ($d\pi(Ir) \rightarrow \pi^*(C^\wedge N)$) transition (see **Table 1**) is

slowly shifted to 356 nm resulting in two isosbestic points at 322 and 360 nm, indicating strong interactions between **1** and the Hg^{2+} ions (**Fig. S15**). A continuous decrease in the absorption intensity at 340 nm for the addition of up to 15μM of Hg^{2+} is

5 observed, while further addition of Hg^{2+} induces only very minor changes in A_{340}, indicating that **1** has a 1:1 interaction[20] with the Hg^{+2} ions (**Fig. S16**). The titration experiment was also performed with the help of photoluminescence spectroscopy. In this case, the emission spectra of **1** are gradually decreasing after

10 addition of Hg^{+2} to the solution (**Fig. 8**). A linear relationship was obtained between I_{463} and the concentration of Hg^{+2} ions between 0 to 6μM, indicating the sensitivity of **1** towards Hg^{+2}. The limit of detection was calculated[14c, 21] to be 170 nM, based on $3\sigma /m$, where σ corresponds to the standard deviation of the blank

15 measurements, and m is the slope in the plot of the intensity versus the sample concentration. This value is reasonably good in comparison to many other reported[5d,7, 22] iridium(III) based Hg^{+2} chemodosimeter [23].
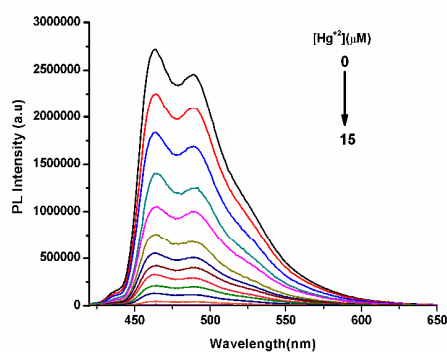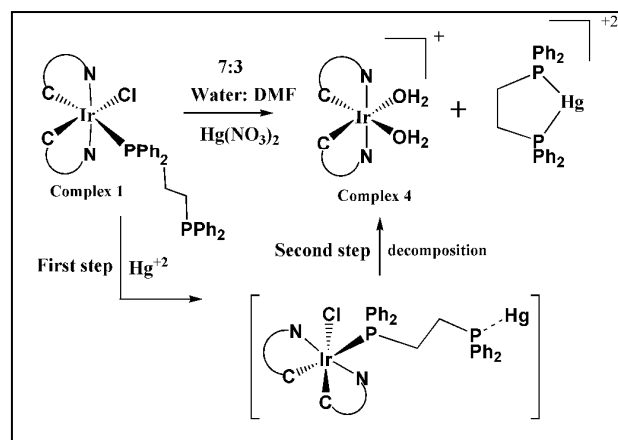
a
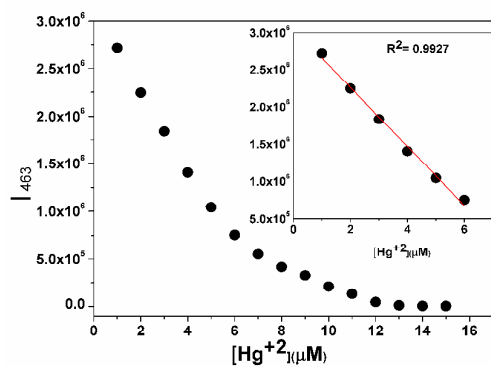
b

Fig. 8 (a) The luminescent spectral changes of complex 1 (fw = 70 %

with [M] $=10^{-5}$ mol L^{-1}) upon the increasing addition of Hg^{+2} ions (from
25 0.0 to 14.0 μM) (nitrate salt). DMF–H_2O (3:7 v/v). λ_{ex} = 380 nm. (b) The plot of I_{463} vs. the concentration of Hg^{+2}; inset, the linear relation of I_{463} vs. the concentration of Hg^{+2} in the range of 0.0–6.0 μM.

The Sensing of Mechanism of Hg^{+2} by complex 1

Scheme 2

30

According to Pearson's hard-soft acid-base theory[6], Hg^{+2} is a soft ion (soft acid) that will interact preferentially with a soft base. A
35 glimpse at previous reports shows that the most widely used soft base is sulphur, whose lone pair can interact with Hg^{+2} ions very easily. According to Hui Zeng *et al.*, lone pairs on nitrogen can also interact with Hg^{+2} forming soft acid base complexes[6]. Herein, we report the first iridium(III) phosphine complex that
40 can be used as a chemodosimeter for low level detection of Hg^{+2}. The synthesized iridium(III) complexes have a free lone pair on the non-coordinated phosphorous atom that can easily interact with Hg^{+2} ions. The interaction of **1** with Hg^{+2} was studied by NMR using different nuclei such as ^1H, ^{31}P and ^{19}F (**Fig. S17-18**).
45 To the Hg-probing mechanism, the interaction of dppe ligand (PPh_2 ligand) with Hg^{+2} has been investigated. The ^1H and ^{31}P NMR spectra of P^P ligand with 2 equivalents mercuric nitrate were taken and compared these with the spectra obtained of P^P ligand without mecuric nitrate (**Fig. S17 a{C, D}, b{C, D}**). It is
50 clearly seen from the ^1H NMR spectrum that the aromatic peaks gets deshielded in case of the mixture of mecuric nitrate and P^P ligand (the signal ~7.29 ppm is shifted to ~7.64 ppm). Similarly, the chemical shift for ^{31}P of P^P-ligand after addition of 2 equivalents mercuric nitrate is moved to more deshielded region
55 (from −14.59 ppm to 38.80 ppm). These downfield proton and phosphorous signals hint that the interaction is being operated

between P^P ligand with mercuric ion. Further, the ^{1}H NMR spectrum of **1** with two equivalents of mercuric nitrate produces a new signal in between 7.52 ppm and 7.79 ppm (which is not observed in ^{1}H NMR spectrum of pure complex **1**, **Fig. S17a{A, B}**). Further, a signal in the similar position (~7.64 ppm) has been observed in the mixture of P^P-ligand and mercuric nitrate (2 equivalents, **Fig. S17a{C}**). These changes in ^{1}H and ^{31}P NMR spectra of complex **1** and P^P-ligand in absence and presence of mercuric nitrate clearly supports the appended P^P-ligand in **1** is involved in interaction with the mercuric ion. Again, the HRMS data for the mixture of complex **1** and mercuric nitrate (1:1) indicates the isolation of several fragments of $[(Ir(F_2ppy)_2(PPh_2CH_2CH_2PPh_2Hg)]^{2+}$ (**Fig. S17c**). In UV-VIS spectrum, the gradual variation of absorbance with increasing concentration of mercuric ion clearly supports 1:1 interaction (**Fig. S16**). All these experimental results tentatively suggest that in the sensing mechanism where mercuric ion can be easily interacted with the appended P^P in complex **1** and at the initial stage, there has formed an intermediate complex, $[(Ir(F_2ppy)_2(PPh_2CH_2CH_2PPh_2Hg)]^{2+}$ (**Scheme 2**). Further, after addition of four equivalents of Hg^{+2} salt in **1**, the luminescent intensity was quenched and a new complex was isolated from the solution by extraction using DCM and water which was characterized by ^{1}H NMR. The ^{1}H NMR spectra of the isolated complex are shown less number of signals as the parent compound **1** (**Fig. 9**). The signal of the diphenyl substituents in the appended diphosphine ligand disappear (^{1}H NMR signal between δ=6.2-7.3 ppm) which evidences the detachment of PPh₂-ligand from the complex resulting a bis-aqua iridium complex[25] [$Ir(F_2ppy)H_2O)_2]^+$, **4** (Scheme 2). To confirm the absence of phosphorus in **4**, it was further studied by ^{31}P NMR spectroscopy which clearly supports the absence of phosphorous in this complex [no P peak at δ= –8.90 ppm – (–12.60 ppm)] (**Fig. S18a**). In addition, the IR spectrum of **4** clearly indicates the presence water molecules (**Fig. S18b**). This mechanism was further supported by ESI-HRMS measurements on a mixture of complex **2** and 4.0 equiv of mercuric nitrate. The original peak at m/z 1006.1608 assigned to complex **1** disappeared and new signals were observed at m/z 573.0561 and 614.0826 which attributes to $[Ir(F_2ppy)_2]^+$ and $[Ir(F_2ppy)_2(ACN)]^+$, respectively (**Fig.S18c**).

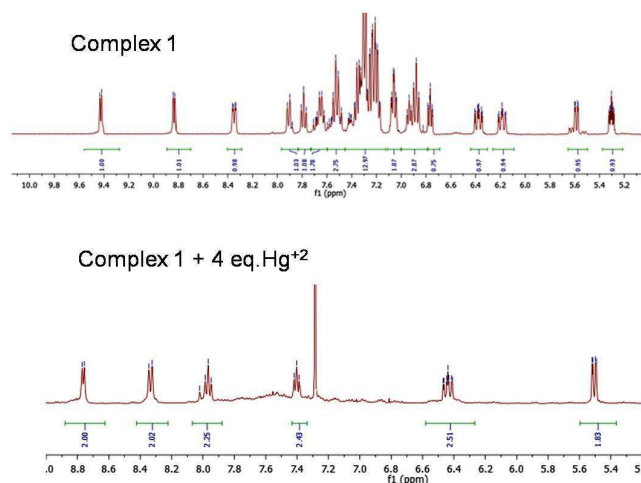**Fig. 9** ^{1}H NMR spectra of **1** (Top) and after addition of 4 eq. of Hg^{+2} to **1** (below)

From the above analysis it can be concluded that the *cis*-bis-aqua complex $[Ir(F_2ppy)(H_2O)_2]^+$ is formed. The ^{1}H NMR spectrum of **4** in CDCl₃ shows six proton signals that match well with $[(F_2ppy)_2Ir(H_2O)_2]^+$ (**Fig. 9**) and the ^{19}F NMR peaks at δ= -107.07 ppm and δ= -109.72 ppm (**Fig. S18d**) reveal its symmetrical geometry (*cis*-C,C complex). ^{31}P NMR spectrum of the mixture of P^P with Hg^{2+} (2 equivalents) result only one signal [**Fig. S17b (C)**]. This observation suggests the symmetrical nature of the detached diphosphine-Hg complex[24] from **1**. From the above discussion, the detached diphosphine-Hg complex from **1** can be tentatively assigned to $[Hg(P^P)]^{2+}$. The FTIR peak of **1** mixed with 2 equivalents of mercuric nitrate resulted a peak at 1280cm⁻¹, in addition to observation of an another peak at 1380cm⁻¹ [**Fig. S17d(iii)**]. The later peak (1380cm⁻¹) matches well with the free mercuric nitrate which remains as in excess in the mixture [**Fig. S17d(i)**]. The other peak observed at 1280cm⁻¹ corresponds to the mono-coordinated nitrate to mercury-diphosphine complex. Further, the HRMS fragment mass of m/z = 666 (m/2) which corresponds to iridium-P^P-Hg(NO₃)₂ complex [**Fig. S17(c)**]. These experiments helped us to assign the structure of detached Hg-diphosphine complex from **1** to $(PPh_2CH_2CH_2PPh_2)Hg(NO_3)_2$.

Conclusions

In summary, we have demonstrated a quite simple reaction route for the syntheses of new blue emitting AIE active iridium(III) complexes with appended free phosphorous atoms that

selectively interact with Hg^{+2} ions and has been used in the efficient detection of mercury(II) ion from environmental samples. The detection limit of mercury(II) from solution went to 170 nM which demonstrates the efficiency of the probe molecules as mercury(II) sensors. Hence, these types iridium based probe molecules can be considered as an efficient chemodosimeter for Hg^{+2}.

Acknowledgements

Reference

1 (a) S. Lamansky, P. Djurovich, D. Murphy, F. Abdel-Razzaq, H. E. Lee, C. Adachi, P. E. Burrows, S. R. Forrest and M. E. Thompson, *J. Am. Chem. Soc.*, 2001, **123**, 4304–4312; (b) A. B. Tamayo, S. Garon, T. Sajoto, P. I. Djurovich, I. M. Tsyba, R. Bau and M. E. Thompson, *Inorg. Chem.*, 2005, **44**, 8723–8732; (c) S.-J. Yeh, M.-F. Wu, C.-T. Chen, Y.-H. Song, Y. Chi, M.-H. Ho, S.-F. Hsu and C. H. Chen, *Adv. Mater.*, 2005, **17**, 285–289; (d) K. K.-W. Lo, C.-K. Chung and N. Zhu, *Chem.–Eur. J.*, 2006, **12**,1500–1512; (e) Q. Zhao, S. J. Liu, M. Shi, C. M. Wang, M. X. Yu, L. Li, F. Y. Li, T. Yi and C. H. Huang, *Inorg. Chem.*, 2006, **45**, 6152–6160; (f) X. H. Li, Z. Chen, L. Shen, F. Y. Li, Q. Zhao, Y. Tao, Y. Cao and C. H. Huang, *Inorg. Chem.*, 2007, **46**, 5518–5527; (g) M. X. Yu, Q. Zhao, L. X. Shi, F. Y. Li, Z. G. Zhou, H. Yang, Y. Tao and C. H. Huang, *Chem. Commun.*, 2008, 2115–2117; (h) Q. Zhao, F. Li, and C, Huang, *Chem. Soc. Rev.*, 2010, **39**, 3007–3030.

2 M. L. Ho, F. M. Hwang, P. N. Chen, Y. H. Hu, Y. M. Cheng, K. S. Chen, G. H. Lee, Y. Chi and P. T. Chou, *Org. Biomol. Chem.*, 2006, **4**, 98–103.

3 (a) D. W. Boening, *Chemosphere.*, 2000, 40, 1335–1351; (b) H. H. Harris, I. J. Pickering and G. N. George, *Science*, 2003, **301**, 1203–1203; (c) P. B. Tchounwou, W. K. Ayensu, N. Ninashvili and D. Sutton, *Environ. Toxicol.*, 2003, **18**, 149–175; (d) T. W. Clarkson, L. Magos and G. J. Myers, *N. Engl. J. Med.*, 2003, **349**, 1731–1737.

4 (a) C. Wang and K. M.-C. Wong, *Inorg. Chem.*, 2011, **50**, 5333-5335; (b) Q. Zhao, S. Liu, F. Li,T. Yi and C. Huang, *Dalton Trans.*, 2008, 3836-3840; (c) Y. Wu, H. Jing, Z. Dong, Q. Zhao, H. Wu and F. Li, *Inorg. Chem.*, 2011, **50**, 7412-7420; (d) H.-F. Shi, S.-J. Liu, H.-B. Sun, W.-J. Xu, Z.-F. An, J. Chen, S. Sun, X.-M. Lu, Q. Zhao and W. Huang, *Chem.–Eur. J.*, 2010, **16**,12158-12167.

5 (a) Q. Zhao, T. Y. Cao, F. Y. Li, X. H. Li, H. Jing, T. Yi and C. H. Huang, *Organometallics*, 2007, **26**, 2077–2081; (b) H. Yang, J.J. Qian, L. T. Li, Z. G. Zhou, D. R. Li, H. X. Wu and S. P. Yang, *Inorg.Chim. Acta*, 2010, **363**, 1755–1759; (c) F. Lu, M. Yamamura and T. Nabeshima, *Dalton Trans.*, 2013, **42**, 12093–12100; (d) F.Yan, Q.Mei, L. Wang , B.Tong, Z.Xu, J. Weng , L. Wang , and W.

Huang, *Inorg. Chem. Commu.*, 2012, **22** , 178–181;(e) B. Tong , Y. Zhang , Z. Han , D.Chen and Q.-F. Zhang, *Inorg. Chem. Commu.*, 2013, **28** , 31–36; (f) Y. Liu, M. Li, Q. Zhao, H.Wu, K. Huang, and F. Li, *Inorg. Chem.*, 2011, **50**, 5969–5977.

6 R. G. Pearson, *J. Am. Chem. Soc.*, 1963, **85**, 3533–3539.

7 H. Zeng, F. Yu, J. Dai, H. Sun, Z. Lu, M. Li, Q. Jiang and Y. Huang, *Dalton Trans.*, 2012, **41**, 4878–4883.

8 C. H. Huang, F. Y. Li and W. Huang, Introduction to Organic Light-Emitting Materials and Devices, Press of Fudan University, Shanghai, 2005.

9 (a) P. Alam, M. Karanam, A. R. Choudhury and I. R. Laskar, *Dalton Trans.*, 2012, **41**, 9276–9279; (b) Q. Zhao, L. Li, F. Y. Li, M. X. Yu, Z. P. Liu, T. Yi and C. H. Huang, *Chem. Commun.*, 2008, 685-687; (c) K. W. Huang, H. Z. Wu, M. Shi, F. Y. Li, T. Yi and C. H. Huang, *Chem. Commun.*, 2009, 1243-1245; (d) C. H. Shin, J. O. Huh, M. H. Lee and Y. Do, *Dalton Trans.*, 2009, 6476-6479; (e) G. G. Shan, L. Y. Zhang, H. B. Li, S. Wang, D. X. Zhu, P. Li,C. G. Wang, Z. M. Su and Y. Liao, *Dalton Trans.*, 2012, 41, 523-530.

10 S. J. Lee, K. M. Park, K. Yang and Y. Kang, *Inorg. Chem.*, 2009,**48**, 1030-1037; (b) C.-H. Yang, M. Mauro, F. Polo, S. Watanabe, I. Muenster, R. Frohlich and L. De Cola, *Chem. Mater.*, 2012, **24**, 3684-3695. (c) Y.-C. Chiu, C.-H. Lin, J.-Y. Hung, Y. Chi, Y.-M. Cheng,. K.-W. Wang,.M.-W. Chung, G.-H. Lee, and P.-T. Chou , *Inorg.Chem.*, 2009,**48**, 8164–8172.

11 A. F.Rausch, M. E.Thompson and H. Yersin, *Inorg. Chem.* 2009, **48**, 1928-1937.

12 A.D. Becke, *J.Chem.Phys.*, 1993, **98**,5648-5652.

13 (a) P.J.Hay and W.R. Wadt, *J. Chem. Phys.*, 1985, **82**, 270-283; (b) W.R.Wadt and P.J. Hay, *J. Chem. Phys.*, 1985, **82**,284-298; (c) P.J.Hay, and W.R. Wadt, *J. Chem. Phys.*, 1985, **82**, 299-311.

14 P. Alam,I. R. Laskar, C.Climent, D.Casanova, P. Alemany M. Karanam, A. R.Choudhury, J. R.Butcherd, *Polyhedron*, 2013, **53**, 286–294.

15 (a) C. Jiang , Y.-S. Wen , L.-K. Liu, T.S. A.Hor,Y and K.Yan, *J. Organo. Chem.*, 1999, **590** , 138-148.(b) K.A. Giffin, D. J. Harrison, I. Korobkov, and R. Tom Baker, *Organometallics*, 2013, **32**, 7424−7430. (c) F. Zhang, L. Wang, S.-H. Chang, K.-L. Huang, Y. Chi, W.-Y. Hung, C.-M. Chen, G.-H. Lee and P.-T. Chou, *Dalton Trans.*, 2013, **42**, 7111–7119.

16 M.G. Haghighi, M. Rashidi, S. M. Nabavizadeh, S. Jamali and R. J. Puddephatt, *Dalton Trans.*, 2010, **39**, 11396–11402.

17 H. Tong, Y. Hong, Y. Dong, Y. Ren, M. Ha1ussler, J. W. Y. Lam, K. S. Wong, and B. Z. Tang, *J. Phys. Chem. B*, 2007, **111**, 2000-2007.

18 X. Zhang, Z. Chi, ,X. Zhou, S. Liu,Y. Zhang, and J. Xu, *J. Phys. Chem. C*, 2012, **116**, 23629−23638.

19 X. Zhang, Z. Chi , B.Xu, H. Li, Z.Yang, X. Li, S. Liu, Y. Zhang and J. Xu, *Dyes and Pigments,* 2011, 89, 56-62.

20 L. Zhang, S. Dong and L. Zhu, *Chem. Commun.*, 2007, 1891–1893.

21 L. N. Neupane, J. M. Kim, C. R. Lohani and K.-H. Lee, *J. Mater. Chem.*, 2012, **22**, 4003–4008; (b) M.-H. Yang, P.Thirupathi, and K.-H. Lee, *Org. Lett.*, 2011, **13**, 5028–5031.

22 B.Tong, Q. Mei , M. Lu, *Inorg. Chim. Acta,* 2012, **391,** 15–19.

23   Y. Yang, Q.Zhao, W.Feng, and F. Li, *Chem. Rev.* 2013, **113**, 192−270.

24   S.A.O. Al-Dury and S. A. A.- Jibori   *Orient. J. Chem*., 2012, 28, 5   781-786

25 (a) A. Maity, B. L. Anderson, N. Deligonula and T. G. Gray, *Chem. Sci.*, 2013, **4**, 1175–1181; (b) B. Schmid, F.0. Garces, and R. J. Watts, *Inorg. Chem.*, 1994, **33**, 9-14.
10